Implications for the 1s0d shell of the new two-body interactions USDA and USDB

W. A. Richter[1] *and B. Alex Brown*[2]
[1] Department of Physics, University of the Western Cape, Private Bag X17, Bellville 7535, South Africa, [2] Department of Physics and Astronomy, and National Superconducting Cyclotron Laboratory, Michigan State University, East Lansing, Michigan 48824-1321, USA

Abstract
The new Hamiltonians USDA and USDB for the sd-shell are used to calculate M1 and E2 moments and transition matrix elements, Gamow-Teller beta decay matrix elements and spectroscopic factors for sd-shell nuclei from A=17 to A=39. The results are compared with those obtained with the older USD Hamiltonian and with experiment to explore the interaction sensitivity of these observables. Predictions up to high energies are also tested for ^{26}Mg in a number of cases.

1 Introduction

Two new interactions, USDA and USDB, [1] have recently been obtained from fits of 63 two-body matrix elements and three single-particle energies to more than 608 binding energies and energy levels for the sd-shell nuclei from A=16 to A=40. The energy data set used for USDA and USDB was updated from the one used 25 years ago to obtain the USD interaction based on 47 linear combinations of parameters fitted to 447 energy data with an rms deviation of 150 keV [2]. The energy data has been improved and extended, in particular with more recent data for the neutron-rich sd-shell nuclei. As a consequence the main change from USD to USDA/B in terms of energies of low-lying states involved the most neutron-rich nuclei, and in particular features related to the position of the neutron $0d_{3/2}$ single-particle state around ^{24}O. The new interactions are used for configuration-interaction calculations involving the $0d_{5/2}, 0d_{3/2}$ and $1s_{1/2}$ active orbitals for protons and neutrons. For USDA 30 linear combinations of one- and two-body matrix elements were varied, with the remaining 36 linear combinations fixed at values of a renormalized G-matrix, with a resulting rms deviation between experimental and theoretical energies of 170 keV. For USDB, 56 linear combinations were varied with 10 fixed at the G-matrix values, and with an improved rms deviation of 130 keV. Binding energies and energy levels for all sd-shell nuclei are shown in [3] and compared with experiment where available.

In this work we make extensive comparisons of observables for the low-lying states of many sd-shell nuclei with the results based on the interactions USDA, USDB and USD. Our goal is also to test these Hamiltonians for observables that go to high excitation energy, and for this purpose we choose ^{26}Mg, a nucleus near the middle of the sd shell. The object is to see to what extent and to what excitation energy experimental states can be associated with states calculated in the sd-shell basis. Comparisons are made as examples for a limited number of cases. Rates for the astrophysical rapid-proton capture process depend upon calculations of gamma widths for levels near the proton decay thresholds [4], [5]. This study provides an example of the applicability and the accuracy of calculations limited to the sd shell.

2 Magnetic dipole moments and transitions

Comparison of theory with experiment is shown in Figs. (a) (for 48 magnetic moments) and (b) (for 111 $M1$ transitions). The sign for the magnetic moments of ^{19}O, ^{23}Mg, ^{31}S, not determined by experiment, are taken from theory. Magnetic moments for neutron-rich Ne [6], Na [7] and Mg [8] sd-shell nuclei

are not included here (See Ref. [19]). Use of the effective g-factors obtained from a simultaneous least-square fit to the magnetic moments and M1 transitions leads to a visible improvement for both moments and transitions. In comparing the spin contribution to the M1 matrix elements it has been found that there is a significant scatter for the different Hamiltonians [19]. Even though there are differences between the results for the different Hamiltonians, one cannot say any one of them is better.

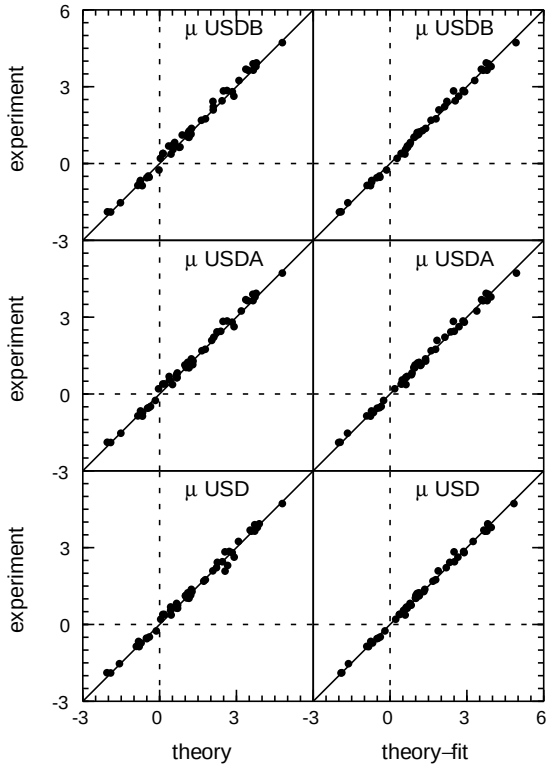

(a) Comparison of experiment and theory for magnetic moments.

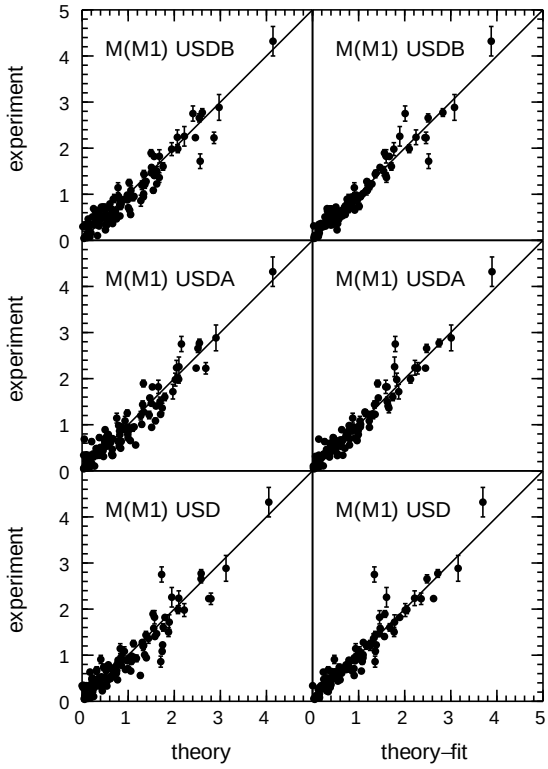

(b) Comparison of experiment and theory for $M1$ transition matrix elements.

3 Electric quadrupole moments and transitions

The two observables are quadrupole moments,

$$Q = \sqrt{\frac{16\pi}{5}} < \Psi \mid (E2)^{op} \mid \Psi >_{M=J}, \tag{1}$$

and $E2$ transition matrix elements,

$$M_p = < \Psi_f || (E2)^{op} || \Psi_i >, \tag{2}$$

related to the $E2$ transition probabilities by $B(E2) = M_p^2/(2J_i + 1)$. We also write these in terms of the explicit proton and neutron components:

$$Q = e_p Q_p + e_n Q_n, \tag{3}$$

and

$$M_p = e_p A_p + e_n A_n. \tag{4}$$

The radial matrix elements were calculated with harmonic-oscillator radial wavefunctions with oscillator lengths fitted to the rms charge radius of the stable isotopes [9].

The result for the three Hamiltonians are compared in Figs. (c) and (d) for both the proton components (Q_p and A_p) and neutron components (Q_n and A_n) of the matrix elements. Except for a few points, the results are remarkably the same. The largest difference shows up in USDB vs USD for A_p and A_n, by the point near the coordinates $(0, 3)$ in the lower panels of Fig. (d). It corresponds to the ^{32}P $4_1^+ \rightarrow 2_1^+$ transition. In the future we will make a complete comparison for odd-odd nuclei such as ^{30}P and ^{34}Cl as a more complete test of the Hamiltonians. For the other cases considered all of the Hamiltonians give essentially the same comparison to data which we show in the top panel of Figs. (c) (for 26 quadrupole moments) and (d) (for 144 $E2$ transitions) for experiment compared to the USDB results.

The least-square fit for the effective charges (with σ_{th} = 2.0 e fm^2) gave essentially the same results for all three Hamiltonians: $e_p = 1.36(5)$ and $e_n = 0.45(5)$. As is well known the effective charge is essential for these $E2$ observables. There is a very large deviation with bare charges (left-hand side of the top panels in Figs. (c) and (d) giving systematically much too small theoretical values. The effective charges reproduce the data with rms deviations of 2.1 e fm^2 for $E2$ transitions and 1.9 e fm^2 for quadrupole moments. Since all three Hamiltonians give essentially the same result for this set of observables, all of the previous analysis obtained with the USD Hamiltonian about the dependence of the effective charges on the assumptions about the radial wavefunctions is still valid [10].

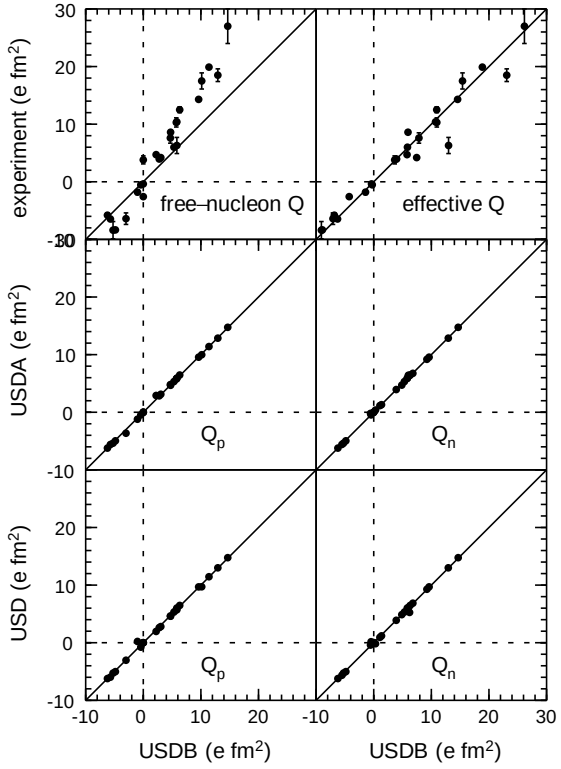

(c) Quadrupole moments. The lower panels show the comparison with the different Hamiltonians. The top panel shows the comparison of experiment with the USDB calculations.

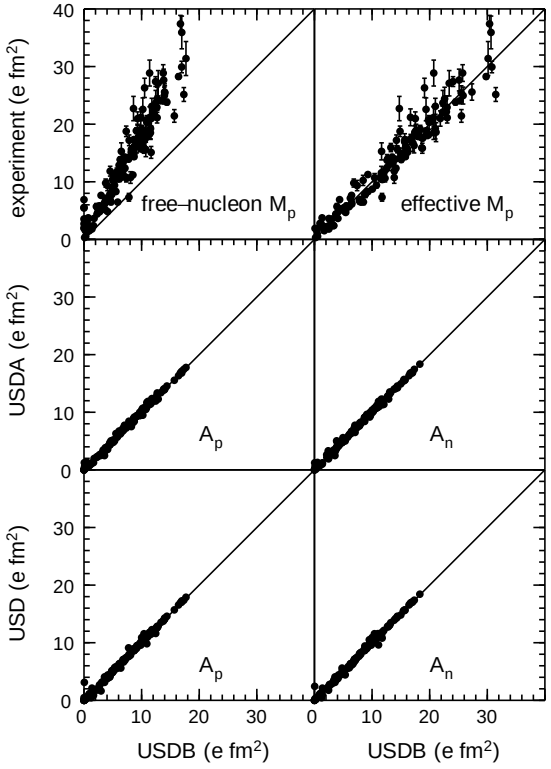

(d) E2 transition matrix elements. The lower panels show the comparison with the different Hamiltonians. The top panel shows the comparison of experiment with the USDB calculations.

4 Gamow-Teller transitions

The Gamow-Teller (GT) beta-decay operator is

$$(GT)^{op} = q_{GT} \Sigma_i 2\, \vec{s}_i\, t_{\pm,i}, \tag{5}$$

where the sum runs over the A nucleons, and $t_\pm$ is the isospin raising-lowering operator. q_{GT} is an effective GT operator (parameter) normalized by its free-nucleon value of $q_{GT} = 1$. The GT transition matrix elements are

$$M(GT) = < \Psi_f || (GT)^{op} || \Psi_i >, \tag{6}$$

related to the GT transition probabilities, $B(GT) = [M(GT)]^2/(2J_i + 1)$.

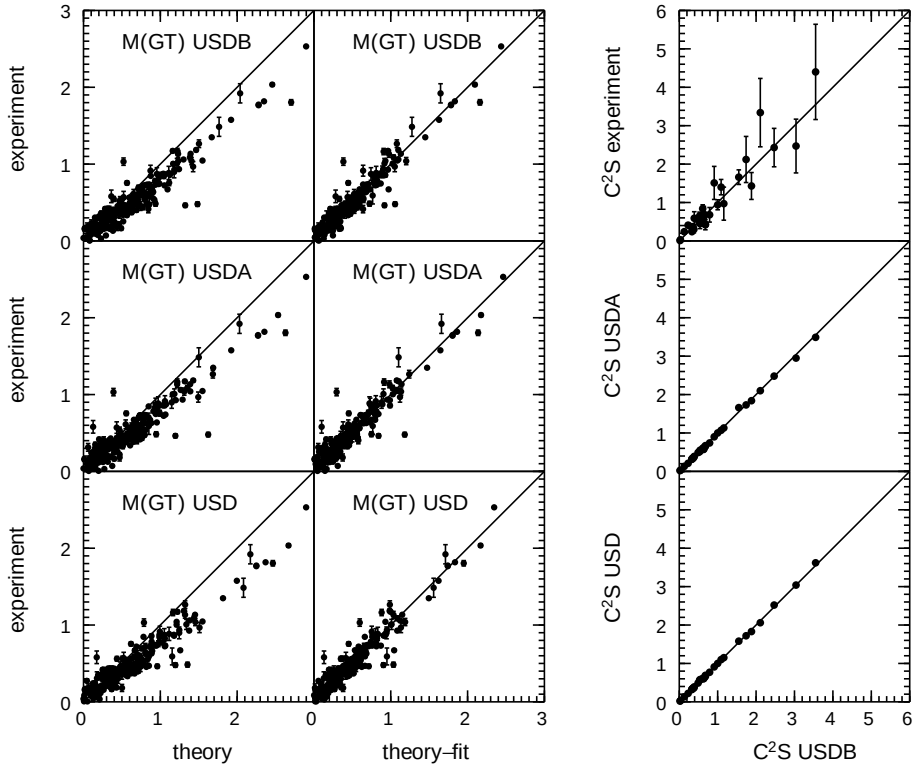

(e) Comparison of experiment and theory for Gamow-Teller decay matrix elements.

(f) A plot of experimental and theoretical single-nucleon spectroscopic factors for the three interactions USD, USDA and USDB.

The $M(GT)$ (with $q_{GT} = 1$) for the matrix elements obtained with the three Hamiltonians show a scatter among the matrix elements, similar to that observed for the $M1$ spin matrix elements, in contrast to the results for $E2$. Thus, we may conclude that the inclusion of $M1$ and GT data in the determination of the Hamiltonian would help to increase the precision of the empirical interaction and its predictive power for $M1$ and GT observables.

The comparison of theory with experiment (232 data) is shown in Fig. (e). The results for the one-parameter fit (σ_{th}=0.15) to q_{GT} give a fairly stable quenching factor with an average of 0.78 . The results for the value of q_{GT} do not depend on the Hamiltonian within the uncertainty, and thus all of the conclusions discussed previously about its interpretation in terms of higher-order configuration mixing and Δ-particle admixtures [10] are still valid.

5 Spectroscopic factors

The results for the basic set of ground state to ground state spectroscopic factors are shown in Fig.(f). The lower two panels compare theory, USDB vs USD and USDB vs USDA. The results are remarkably similar between the calculations. Thus, we only only need to compare them with experiment. The data for spectroscopic factors between ground states are taken from Table I of from Tsang et al [11] (see

also [12]). (The spectroscopic factor of 1.60±0.23 given in Table I of [11] for ^{19}F(p,d)^{18}F appears to be that for the transfer to the 3^+ excited state of ^{18}F. We have replaced this with the value of 0.65±0.10 from [13] obtained for the transfer to the 1^+ ground state.) Experiment is compared with values obtained with the USDB Hamiltonian in the top panel of Fig. (f). The agreement between experiment and theory is good. The spectroscopic factors extracted from the analysis of [11] depends upon the optical potentials. Reasonable changes in the optical potential can lead to reduced values of the extracted spectroscopic factors that are closer to those obtained from $(e, e'p)$ reactions [15], [16].

6 Study of ^{26}Mg

Previous studies of ^{26}Mg have made extensive comparisons of predictions for the older USD interaction to data on ^{24}Mg(p,t)^{26}Mg [17] and high-spin states [18]. Our results are consistent with the level associations made in these works, but add much more in terms of comparison with the more recently derived interactions, and in terms of more recent experimental work especially in regard to data on inelastic excitation. Assignments between theory and experiment of corresponding levels in ^{26}Mg levels have been made based on energies, lifetimes, branching ratios, electron scattering form factors and reduced electromagnetic transition strengths. Results based on the new sd-shell interactions USDA and USDB, as well as the older USD interaction have been compared. Because of a lack of space, we illustrate only some aspects of the assignments and comparisons - a more comprehensive study will be published elsewhere. For the calculation of electromagnetic transition strengths and electron scattering form factors harmonic oscillator radial wave functions with b = 1.769 fm and $\hbar\omega = 13.260$ MeV have been used, and effective charges and g-factors from obtained from fits to large numbers of data (moments as well as transitions) in Ref. [19], unless stated otherwise.

7 Comparison of energies and lifetimes of levels

Up to 8 MeV all experimental positive parity states have a definite spin-parity assignment with the exceptions of the 6.634 MeV (0 to 4)$^+$ state, the 7.200 MeV (0,1)$^+$ state and the 7.816 MeV (2,3)$^+$ state. For the observed 6.634 MeV state theory predicts a 1^+ state in this energy region, and the halflives lie within the observed upper limits. The 7.200 MeV (0,1)$^+$ states does not appear to have a theoretical counterpart and thus may be the first "intruder" positive parity state, related to two nucleons excited from the $0p$-shell or to the $1p0f$ shell. Above 8 MeV there are many experimental states with uncertain spin and/or parity assignments, so the association of experimental and theoretical states above 8 MeV is made on the basis of those selectively populated in electron scattering or beta decay as discussed in the the next sections. The experimental energies in are compared with the USDB energies in Fig. (g).

A significant parameter to consider when assigning theoretical levels to experimental ones, in addition to energy, is the level lifetime. The halflives are based on calculations of all possible decays from a given level (M1 and E2), and were calculated with the programs NuShell and DENS [3]. Effective g-factors and charges determined from least-square fits to a large number of data (moments as well as transitions) have been used [19]. The calculated halflives are based on the theoretical energy levels for the electromagnetic phase-space factors. In most cases the differences obtained if experimental energies were used would be 10% or less. Up to about 7 MeV there is a good correspondence generally between experimental and calculated halflives, and where there are only upper limits for experiment, the theory values lie within the limits. The ratios of experimental to theoretical halflives are plotted in Fig. (h) for the first 21 states of USDB (up to 7.4 MeV experimental energy). Where there are only experimental limits the range of possible ratios are shown as vertical lines. With a few exceptions, particularly where the experimental errors are very large, the ratios of USDA and USDB lie fairly close to the value of 1, indicating good overall agreement between theory and experiment. There is a larger scatter for USD.

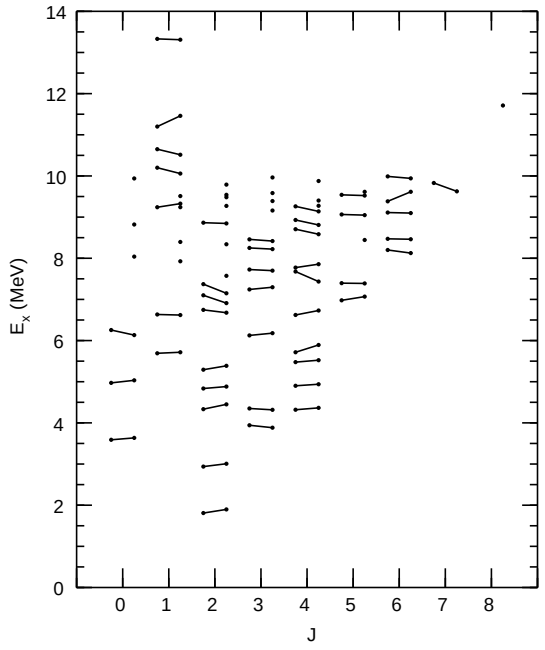

(g) Comparison of experimental energies (left) vs the USDB theoretical energies (right) for positive parity states with angular momentum J . All theoretical levels up to 10 MeV are shown. Levels above 10 MeV correspond to 1^+ states obtained from electron scattering and (γ, γ') reactions, and the lowest 8^+ level.

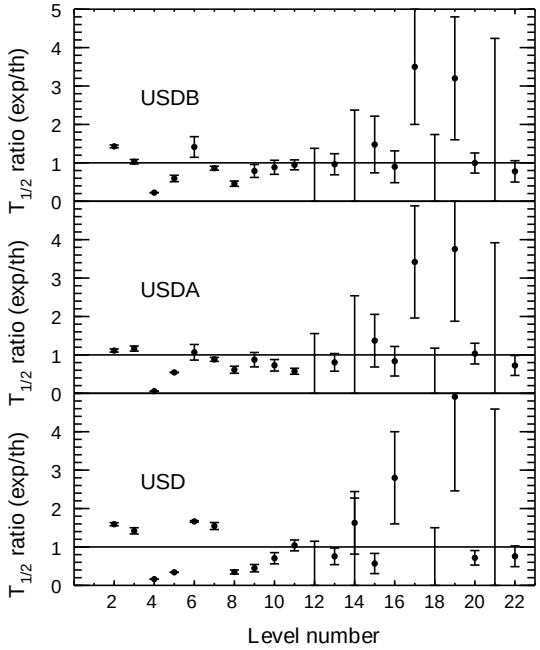

(h) Ratios of halflives versus level number n (for USDB)

8 Comparison with form factors from electron scattering

Inelastic electron scattering to excited states in ^{26}Mg is one of the key methods in making associations between experimental and theoretical energy levels. In the following sections we consider available electron scattering data for states of various spins. Details of the form factor calculations are given in [20] for E2 and E4, and [21] for M1, M3 and M5. For E2 and E4 we use the Tassie-model form factor for the core-polarization contribution [20]. For these multipoles the shape and the experimental and theoretical form factors are similar up through the first minimum. Thus for making comparisons between experimental and theoretical strengths is it practical to compare the magnitude of the first maximum in the respective form factors. The error bars are generally small and only indicated if significant.

8.1 Scattering to 3^+ states

Electron scattering from the 0^+ ground state of ^{26}Mg to 3^+ states have provided assignments of several new 3^+ states. Form factors and a set of B(M3) values are given in refs. [22], [23]. (An eighth 3^+ state was assigned to an observed level at 9.042 MeV in ref. [22], but an assignment of 2^- was made for this state in ref. [23].)

The magnitudes of the first maxima of the transverse form factors are compared in Fig. (i) with values from the new interactions USDA and USDB, as well as with the USD interaction, using free-nucleon g-factors. The vertical bins serve as a guide to the eye. For the first seven states, up to 9 MeV, it is evident that there is an unambiguous correspondence between experiment and theory. Above 9 MeV the calculated M3 strength is small and it is evident that some of the states predicted are too weak to be observed experimentally.

It was claimed in Ref. [22] that no overall quenching of in the $B(M3)$ strength had been found. However, as we have used free-nucleon g-factors it is evident from Fig. (i) that there is some quenching

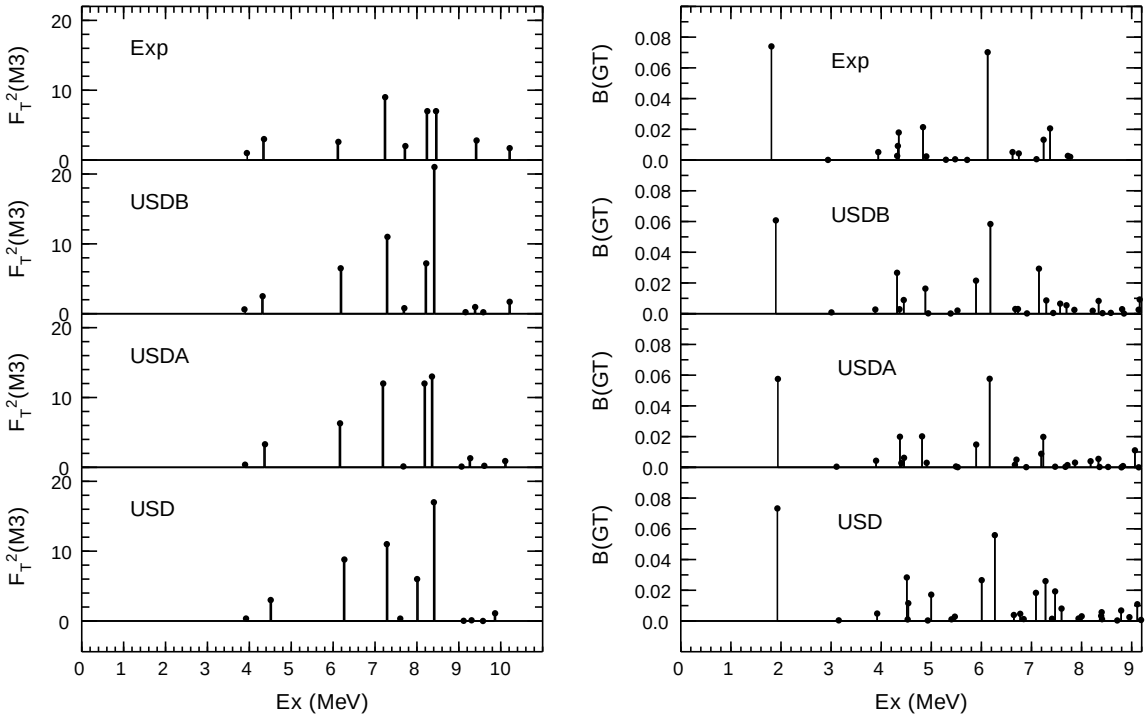

(i) Comparison of the first maxima of the experimental transverse form factors F_T^2(M3) (multiplied by 10^6) with values from the interactions USDA, USDB and USD. (j) Comparison of experimental $B(GT)$ values from Ref. [24] with values from the interactions USDA, USDB and USD. Free-nucleon g-factors have been used.

at the peak of the first maximum in the $M3$ form factors. The quenching factors for the summed strength is given respectively by 0.73 (USDA), 0.69 (USDB) and 0.76 (USD).

9 Results for Gamow-Teller strengths of beta decay of ^{26}Na to states in ^{26}Mg.

High-precision measurements of the half-life and β-branching ratios for the β^- decay of ^{26}Na to ^{26}Mg have been made in β-counting and γ-decay experiments respectively [24]. B(GT) values for decays from the 3^+ ground state of ^{26}Na to 2^+, 3^+ and 4^+ states were extracted from the *ft* values determined, and are compared with the different interactions in Fig. (j). We used effective operators for the calculated Gamow-Teller matrix elements with q_{GT} given in Ref. [19]. There is a good general correspondence between theory and experiment, with USDA giving the best overall agreement.

10 Conclusions

We have used three sd-shell Hamiltonians (USD, USDA and USDB) to investigate observables that include $M1$ moments and $M1$ transition matrix elements, $E2$ moments and $E2$ transition matrix elements, Gamow-Teller beta decay matrix elements and spectroscopic factors between ground states. For nuclei near stability all of these Hamiltonians give a similar description of the energies, whereas the recent USDA and USDB are better for energies of neutron-rich sd-shell nuclei. Some linear combinations of two-body matrix elements are not well determined from the energy data and must be replaced by theoretical values based on renormalized G-matrix approximations. Thus, the predictions for these observables which depend upon the Hamiltonian, provide a discriminating test, and may lead to ways to further constrain the Hamiltonian and to improve the wavefunctions. Such improvements would decrease the uncertainties for the applications to nuclear astrophysics where the needed reaction rates depend entirely

or in part on theoretical input for gamma widths and spectroscopic factors [5].

Using the new sd-shell interactions USDA and USDB, as well as the older USD interaction, assignments between theory and experiment of corresponding levels in ^{26}Mg levels have been confirmed, and new ones suggested. Excitation energies up to about 10 MeV have been considered, and in some cases even higher energies, based on electron scattering data and electromagnetic transition strengths. Level lifetimes based on the detailed gamma decay transition schemes have also been provided. We have been able to make the association of theoretical levels to about 50 experimental levels. Overall the new interactions USDA and USDB are better than USD with regard to detailed comparison with data. The differences between USDA and USDB appear to provide a reasonable estimate of the theoretical error in predicting the observables and we recommend that they both be used for future comparison to experiment and astrophysical applications.

Acknowledgments This work is partly supported by NSF Grant PHY-0758099 and the National Research Foundation of South Africa under Grant No. 2073007.

References

[1] B. A. Brown and W. A. Richter, Phys. Rev. C **74**, 034315 (2006).

[2] B. H. Wildenthal, Prog. Part. Nucl. Phys. **11**, 5 (1984).

[3] B. A. Brown et al., http://www.nscl.msu.edu /˜brown/resources/resources.htm.

[4] H. Herndl, J. Goerres, M. Wiescher, B. A. Brown and L. Van Wormer, Phys. Rev. C **52**, 1078 (1995).

[5] H. Schatz, C. A. Bertulani, B. A. Brown, R. R. C. Clement and B. M. Sherrill, Phys. Rev. C **72**, 065804 (2005).

[6] W. Geithner et al., Phys. Rev. C **71**, 064319 (2005).

[7] G. Huber et al., Phys. Rev. C **18**, 2342 (1978).

[8] M. Kowalska et al., Phys. Rev. C **77**, 034307 (2008).

[9] B. A. Brown, W. Chung and B. H. Wildenthal, Phys. Rev. C **22**, 774 (1980).

[10] B. A. Brown and B. H. Wildenthal, Ann. Rev. of Nucl. Part. Sci. **38**, 29 (1988).

[11] M. B. Tsang, Jenny Lee and W. G. Lynch, Phys. Rev. Lett. **95**, 222501 (2005).

[12] J. Lee, M. B. Tsang and W. G. Lynch, Phys. Rev. C **75**, 064320 (2007).

[13] J. M. Delbrouck-Habaru and G. Robaye, Nucl. Phys. **A337**, 107 (1980).

[14] A. Gade et al., Phys. Rev. C 77, 044306 (2008).

[15] G. J. Kramer, H. P. Blok and L. Lapikas, Nucl. Phys. **A679**, 267 (2001).

[16] J. Lee, J. A. Tostevin, B. A. Brown, F. Delaunay, W. G. Lynch, M. J. Saelim and M. B. Tsang, Phys. Rev. C **73**, 044608 (2006).

[17] W. P. Alford, J. A. Cameron, E. Habib and B. H. Wildenthal, Nucl. Phys. **A454**, 189 (1986).

[18] F. Glatz et al., Z. Phys. A **324**, 187 (1986).

[19] W. A. Richter, S. Mkhize and B. A. Brown, Phys. Rev. C **78**, 064302-1 (2008).

[20] B. A. Brown, R. Radhi and B. H. Wildenthal, Physics Reports C **101**, 313 (1983).

[21] B. A. Brown, B. H. Wildenthal, C. F. Williamson, F. N. Rad, S. Kowalski, J. Heisenberg, H. Crannell and J. T. O'Brien, Phys. Rev. C **32**, 1127 (1985).

[22] K. K. Seth, R. Soundranayagam, A. Saha, C. W. de Jager, H. de Vries, B. A. Brown and B. H. Wildenthal, Phys. Rev. Lett. 74, 642 (1995).

[23] R. Soundranayagam, K. K. Seth, A. Saha, M. Sarmiento, C. W. de Jager, H. de Vries, G. van der Steenhoven, B. A. Brown and B. H. Wildenthal, private communication.

[24] G. F. Grinyer et al, Phys. Rev. C **71**, 044309 (2005).